DESY 13-015
MPP-2013-291

Implications of LHC search results on the W boson mass prediction in the MSSM

S. Heinemeyer[1*], W. Hollik[2†], G. Weiglein[3‡], and L. Zeune[3§]

[1]*Instituto de Física de Cantabria (CSIC-UC), Santander, Spain*
[2]*Max-Planck-Institut für Physik (Werner-Heisenberg-Institut), Föhringer Ring 6, D–80805 München, Germany*
[3]*DESY, Notkestraße 85, D–22607 Hamburg, Germany*

arXiv:1311.1663v1 [hep-ph] 7 Nov 2013

Abstract

We present the currently most precise W boson mass (M_W) prediction in the Minimal Supersymmetric Standard Model (MSSM) and discuss how it is affected by recent results from the LHC. The evaluation includes the full one-loop result and all known higher order corrections of SM and SUSY type. We show the MSSM prediction in the M_W–m_t plane, taking into account constraints from Higgs and SUSY searches. We point out that even if stops and sbottoms are heavy, relatively large SUSY contributions to M_W are possible if either charginos, neutralinos or sleptons are light. In particular we analyze the effect on the M_W prediction of the Higgs signal at about 125.6 GeV, which within the MSSM can in principle be interpreted as the light or the heavy $\mathcal{CP}$-even Higgs boson. For both interpretations the predicted MSSM region for M_W is in good agreement with the experimental measurement. We furthermore discuss the impact of possible future LHC results in the stop sector on the M_W prediction, considering both the cases of improved limits and of the detection of a scalar top quark.

*email: Sven.Heinemeyer@cern.ch
†email: hollik@mpp.mpg.de
‡email: Georg.Weiglein@desy.de
§email: Lisa.Zeune@desy.de

1 Introduction

The recent discovery of a signal with a mass of around 125.6 GeV in the Higgs searches at ATLAS [1] and CMS [2] is compatible with the Higgs boson postulated by the Standard Model (SM), but it can also be interpreted in a variety of models of physics beyond the SM. On the other hand, the direct searches for physics beyond the SM have not resulted in a signal so far. In order to enhance the sensitivity for discriminating between different models of the underlying physics, it is useful to complement the measurements of the properties of the new state with other high-precision observables that have sensitivity to the quantum level, i.e. to loop contributions involving in principle all the particles of the considered model.

In this context, the relation between the W boson mass, M_W, and the Z boson mass, M_Z, in terms of the fine-structure constant, α, the Fermi constant, G_μ, and the parameters entering via loop contributions plays a crucial role. The accuracy of the measurement of the W boson mass has significantly been improved with the latest results presented by CDF [3] and DØ [4]. Together with the results obtained at LEP [5] this gives rise to the latest world average of [6, 7]

$$M_W^{\rm exp} = 80.385 \pm 0.015 \text{ GeV}, \tag{1}$$

i.e. to a relative experimental accuracy of better than 2×10^{-4}. Furthermore, the improved measurement of the top-quark mass, m_t, at the Tevatron and the LHC (see below for a discussion of the physical interpretation of those measurements) has improved the accuracy of the theoretical prediction for M_W, since the experimental error of the input parameter m_t constitutes a dominant source of (parametric) uncertainty in the theoretical prediction, see e.g. Ref. [8]. Further observables that have a high sensitivity for testing electroweak physics at the quantum level are in particular the effective leptonic weak mixing angle at the Z-resonance, $\sin^2\theta_{\rm eff}$, the anomalous magnetic moment of the muon, $(g-2)_\mu$, and rare b decays such as $b \to s\gamma$. The interpretation of the constraints from $\sin^2\theta_{\rm eff}$ are complicated by the fact that the two single most precise measurements, $A_{\rm LR}$ by SLD [7] and $A_b^{\rm FB}$ at LEP [7], differ from each other by more than $3\,\sigma$, see e.g. Ref. [9] for a recent discussion. While the experimental value of $(g-2)_\mu$ shows a significant deviation from the SM prediction at the level of 3–4 σ, which led to many interpretations in terms of new physics models (see e.g. Refs. [10–12] for reviews), the analysis of rare b decays so far has been inconclusive [13].

We will concentrate in the following on the prediction for the W boson mass and, taking into account the latest experimental results, compare the prediction of the SM with that of its most popular extension, the Minimal Supersymmetric Standard Model (MSSM) [14–16]. Within the SM, the interpretation of the discovered new state as the SM Higgs boson implies that there is no unknown parameter anymore in the prediction for M_W. This fact considerably sharpens both the comparison with the experimental result for M_W and with predictions in extensions of the SM such as the MSSM. Our analysis within the MSSM updates previous studies, see in particular Refs. [17, 18] and references therein. Our results are based on the currently most precise prediction for M_W in the MSSM, which we compare with the result in the SM. The MSSM prediction consists of a complete one-loop calculation for the general case of complex parameters (without flavor violation in the sfermion sector [19]), combined with all known higher-order corrections of SM and supersymmetric (SUSY) type. Compared to the result employed in Ref. [17], the MSSM prediction used in the present analysis has

been improved in several respects: the one-loop result in the MSSM has been reevaluated and coded in a more flexible way, which permits an improved treatment of regions of parameter space that can lead to numerical instabilities and furthermore provides the functionality to easily implement results for non-minimal SUSY models (see Ref. [20] and also Ref. [21] for the case of the NMSSM); the incorporation of the state-of-the-art SM result has been improved using the expressions given in Ref. [22].

The top quark mass used in our evaluation corresponds to the pole mass. In our results it could easily be re-expressed in terms of a properly defined short distance mass such as the $\overline{\rm MS}$ or $\overline{\rm DR}$ mass. The parameter measured with high precision via direct reconstruction at the Tevatron and the LHC is expected to be close to the top pole mass, and we adopt this interpretation in the following. For a discussion of the systematic uncertainties arising from the difficulties how to relate the measured mass parameter to the pole mass see Refs. [23, 24].

Extensive searches for SUSY particles have been performed by ATLAS and CMS. No supersymmetric particles have been detected so far in direct searches, and stringent limits were set in particular on the gluino mass and the mass of the squarks of the first two generations [25–28], see however Refs. [29, 30]. Substantially weaker limits have been reported for the particles of the other MSSM sectors, so that third-generation squarks, stops and sbottoms, as well as the uncolored SUSY particles are significantly less constrained by LHC searches, and LEP limits still give relevant constraints [31].

In this paper we analyze the prediction for M_W in view of the discovery of a signal in the Higgs searches at ATLAS and CMS. Within the framework of the MSSM the lighter $\mathcal{CP}$-even Higgs boson can have a mass of about 125.6 GeV for sufficiently large M_A and sufficiently large higher-order corrections from the scalar top sector. It is interesting to note that a mass value as high as about 125.6 GeV for the lighter $\mathcal{CP}$-even Higgs boson of the MSSM implies that M_A has to be in the decoupling region, $M_A \gg M_Z$, which in turn has the consequence that the state at about 125.6 GeV has a SM-like behavior, see e.g. the discussion in Refs. [32, 33]. However, also the interpretation of the discovered particle as the heavy $\mathcal{CP}$-even Higgs state of the MSSM is, at least in principle, a viable possibility, see Refs. [32–38][1]. We take into account the information from the mass measurement of the observed Higgs boson for these two cases, and for the light Higgs interpretation we investigate the correlation between M_W and $\Gamma(h \to \gamma\gamma)$. The limits from Higgs searches at LEP, the Tevatron and the LHC are incorporated with the help of the code `HiggsBounds` (version 4.0.0) [40–42][2]. We perform scans over the relevant SUSY parameters and we analyze in detail the impact of different SUSY sectors on the prediction of M_W. We also investigate possible effects of either future limits from SUSY searches at the LHC or of the detection of a scalar top quark.

This paper is organized as follows: In the next section we give a short summary of the relevant MSSM sectors and specify our notation. In Sect. 3 and 4 we describe the evaluation of M_W in the MSSM. In Sect. 5 we present the result for M_W from a global scan over the MSSM parameter space. We investigate the contributions from all relevant MSSM particle sectors and analyze the impact of the observed Higgs signal as well as from limits arising from searches for Higgs bosons and SUSY particles. Effects of possible future results from

[1] This scenario is challenged by the recent ATLAS bound on light charged Higgs bosons [39].

[2] The latest ATLAS results on light charged Higgs boson searches [39] are not included in this `HiggsBounds` version (while finalizing this paper a new `HiggsBounds` version including this result became available [43]).

SUSY searches at the LHC are also discussed in this context. The conclusions can be found in Sect. 6.

2 Particle sectors of the MSSM

The prediction for M_W in the MSSM depends on the masses, mixing angles and couplings of all MSSM particles. Sfermions, charginos, neutralinos and the MSSM Higgs bosons enter already at the one-loop level and can give substantial contributions to M_W. In this section we briefly describe the relevant MSSM sectors and fix our notation for the MSSM parameters. In our numerical analysis below we will focus on the case of real MSSM parameters. For a discussion of the possible impact of non-zero phases of the MSSM parameters see Ref. [17].

Contrary to the SM, two Higgs doublets are required in the MSSM, resulting in five physical Higgs boson degrees of freedom. At the tree level, where possible $\mathcal{CP}$-violating contributions of the soft supersymmetry-breaking terms do not enter, these are the light and heavy $\mathcal{CP}$-even Higgs bosons, h and H, the $\mathcal{CP}$-odd Higgs boson, A, and the charged Higgs bosons, $H^\pm$. At lowest order the MSSM Higgs sector is fully described by M_Z and two MSSM parameters, often chosen as the $\mathcal{CP}$-odd Higgs boson mass, M_A, and $\tan\beta \equiv v_2/v_1$, the ratio of the two vacuum expectation values. Higher-order corrections to the Higgs boson masses can be sizeable and must be included. Particularly important are the one- and two-loop contributions from top quarks and squarks. Accordingly, the masses of the $\mathcal{CP}$-even neutral Higgs bosons and the charged Higgs boson are not free parameters (as the Higgs mass in the SM), but can be predicted in terms of the other MSSM parameters (introduced below).

The sfermion mass matrix in the gauge-eigenstate basis ($\tilde{f}_L$, $\tilde{f}_R$) for one generation and flavor f is given by

$$\mathbf{M}_{\tilde{f}} = \begin{pmatrix} M^2_{\tilde{f}_L} + m_f^2 + M_Z^2 \cos 2\beta (I_3^f - Q_f s_{\rm w}^2) & m_f\, X_f \\ m_f\, X_f & M^2_{\tilde{f}_R} + m_f^2 + M_Z^2 \cos 2\beta Q_f s_{\rm w}^2 \end{pmatrix} . \tag{2}$$

Here m_f denotes the corresponding fermion mass, I_3 is the third component of the weak isospin, Q_f the electric charge and $s_{\rm w}$ is the sine of the weak mixing angle. The L–R mixing of the sfermions is determined by the off-diagonal entries

$$m_f X_f = m_f (A_f - \mu \{\cot\beta, \tan\beta\}), \tag{3}$$

where $\cot\beta$ refers to up-type sfermions and $\tan\beta$ to down-type sfermions. A_f denotes the trilinear Higgs-sfermion coupling and μ the Higgsino mass parameter. The SUSY-breaking parameters are:

$$M_{\tilde{f}_L} = \begin{cases} M_{\tilde{Q}_i} & \text{for left-handed squarks} \\ M_{\tilde{L}_i} & \text{for left-handed sleptons} \end{cases} \tag{4}$$

$$M_{\tilde{f}_R} = \begin{cases} M_{\tilde{U}_i} & \text{for right-handed u-type squarks} \\ M_{\tilde{D}_i} & \text{for right-handed d-type squarks} \\ M_{\tilde{E}_i} & \text{for right-handed charged sleptons} , \end{cases} \tag{5}$$

where $i = 1, 2, 3$ is the family index. Flavor violation in the sfermion sector is neglected here (see Refs. [19, 44] for a discussion of this kind of effects in the one-loop contributions to M_W). The charged gauginos and Higgsinos mix with each other, yielding charginos $\tilde{\chi}^{\pm}_{1,2}$. The corresponding mass matrix is given by

$$\mathbf{M}_{\tilde{\chi}^{\pm}} = \begin{pmatrix} M_2 & \sqrt{2} M_W \sin\beta \\ \sqrt{2} M_W \cos\beta & \mu \end{pmatrix} , \tag{6}$$

with the soft breaking parameter M_2. The neutralinos are mixtures of the neutral gauginos and Higgsinos. The neutralino mass matrix in the basis $(\tilde{B}, \tilde{W}^0, \tilde{H}^0_1, \tilde{H}^0_2)$ is given by

$$\mathbf{M}_{\tilde{\chi}^0} = \begin{pmatrix} M_1 & 0 & -M_Z s_\mathrm{w} \cos\beta & M_Z s_\mathrm{w} \sin\beta \\ 0 & M_2 & M_Z c_\mathrm{w} \cos\beta & -M_Z c_\mathrm{w} \sin\beta \\ -M_Z s_\mathrm{w} \cos\beta & M_Z c_\mathrm{w} \cos\beta & 0 & -\mu \\ M_Z s_\mathrm{w} \sin\beta & -M_Z c_\mathrm{w} \sin\beta & -\mu & 0 \end{pmatrix} . \tag{7}$$

The gluino is the only SUSY particle that enters only from the two-loop level onwards; thus the impact of the gluino mass, $m_{\tilde{g}} = |M_3|$, on the M_W prediction is relatively small.

3 Determination of the W boson mass

Muons decay via the weak interaction almost exclusively into $e\bar{\nu}_e\nu_\mu$ [31]. The decay was originally described within the Fermi model, which is a low-energy effective theory that emerges from the SM in the limit of vanishing momentum transfer. The Fermi constant, G_μ, is determined with high accuracy from precise measurements of the muon life time [45] and the corresponding Fermi-model prediction including QED corrections up to $O(\alpha^2)$ for the point-like interaction [46–50]. Comparison of the muon-decay amplitude in the Fermi model and in the SM or extensions of it yields the relation

$$\frac{G_\mu}{\sqrt{2}} = \frac{e^2}{8 s_W^2 M_W^2} \left(1 + \Delta r\right) . \tag{8}$$

Here Δr represents the sum of all contributing loop diagrams to the muon-decay amplitude after splitting off the Fermi-model type virtual QED corrections,

$$\Delta r = \sum_i \Delta r_i \, , \tag{9}$$

with

$$\mathcal{M}_{\mathrm{Loop,i}} = \Delta r_i \, \mathcal{M}_{\mathrm{Born}} \, . \tag{10}$$

This decomposition is possible since after subtracting the Fermi-model QED corrections, masses and momenta of the external fermions can be neglected, which allows to reduce all loop contributions to a term proportional to the Born matrix element, see Refs. [51, 52]. By rearranging Eq. (8), the W boson mass can be calculated via

$$M_W^2 = M_Z^2 \left(\frac{1}{2} + \sqrt{\frac{1}{4} - \frac{\alpha\pi}{\sqrt{2} G_\mu M_Z^2} \left(1 + \Delta r\right)} \right) . \tag{11}$$

In different models, different particles can contribute as virtual particles in the loop diagrams to the muon-decay amplitude. Therefore, the quantity Δr depends on the specific model parameters, and Eq. (11) provides a model-dependent prediction for the W boson mass. The quantity Δr itself does depend on M_W as well; hence, the value of M_W as the solution of Eq. (11) has to be determined numerically. In practice this is done by iteration. In most cases this procedure converges quickly and only a few iterations are needed.

In order to exploit M_W as a precision observable providing sensitivity to quantum effects it is crucial that the theoretical predictions for Δr are sufficiently precise with respect to the present and expected future experimental accuracies of M_W. Within the SM the full one-loop [51, 53] and two-loop [52, 54–64], as well as the leading higher-order corrections [65–73] are known. In addition a convenient fitting formula for M_W containing all numerically relevant contributions has been developed [74], and in Ref. [22] a corresponding formula for the two-loop electroweak contributions to Δr has been given. In the MSSM the one-loop result [17, 75–85] and leading two-loop corrections have been obtained [86–89].

4 Calculation of Δr

Our analysis is based on a new one-loop calculation of Δr in the MSSM with complex parameters which has been carried out using the `Mathematica` [90] based programs `FeynArts` (Version 3.5) [91–96] and `FormCalc` (Version 6.2) [97], see Ref. [20] for further details. The one-loop result is combined with all known higher order corrections of SM and SUSY type as specified below, so that the numerical results given in this paper correspond to the currently most precise predictions for the W boson mass in the SM and the MSSM.

4.1 One-loop calculation in the MSSM

The one-loop contributions to Δr consist of the W boson self-energy, vertex and box diagrams, and the related counter terms (CT),

$$\begin{aligned}\Delta r \;&=\; W \text{ Self-energy} + W \text{ Self-energy CT} + \text{Vertex} + \text{Vertex CT} + \text{Box} \\ &= \frac{\Sigma_T^{WW}(0)}{M_W^2} + \left(-\delta Z_W - \frac{\delta M_W^2}{M_W^2}\right) + \text{Vertex} \\ &+ \left(2\delta Z_e - 2\frac{\delta s_\mathrm{w}}{s_\mathrm{w}} + \delta Z_W + \frac{1}{2}\left(\delta Z^\mu + \delta Z^e + \delta Z^{\nu_\mu} + \delta Z^{\nu_e}\right)\right) + \text{Box}\,.\end{aligned} \tag{12}$$

Here Σ_T denotes the transverse part of a gauge boson self-energy, δM_W is the counter-term for the W boson mass, δZ_e and δs_w are the renormalization constants for the electric charge and the (sine of the) weak mixing angle, respectively, while the other δZ denote field renormalization constants. Since the W boson appears only as a virtual particle, its field renormalization constant δZ_W drops out in the Δr formula. The box diagrams are themselves UV-finite in a renormalizable gauge. Choosing on-shell renormalization conditions,[3] which

[3]The on-shell renormalization conditions correspond to the definition of the W and Z boson masses according to the real part of the complex pole of the propagator. This gives rise to the fact that the

ensures that Eq. (8) corresponds to the relation between the physical masses of the W and Z bosons, yields (neglecting the masses of the external fermions)[4]

$$\begin{aligned}\Delta r =& \frac{\Sigma_T^{WW}(0) - \mathrm{Re}\left(\Sigma_T^{WW}(M_W^2)\right)}{M_W^2} + \Pi^{AA}(0) - \frac{c_\mathrm{w}^2}{s_\mathrm{w}^2}\,\mathrm{Re}\left[\frac{\Sigma_T^{ZZ}(M_Z^2)}{M_Z^2} - \frac{\Sigma_T^{WW}(M_W^2)}{M_W^2}\right] \\ &+ 2\,\frac{\mathrm{sgn}\; s_\mathrm{w}}{c_\mathrm{w}}\,\frac{\Sigma_T^{AZ}(0)}{M_Z^2} + \mathrm{Vertex} + \mathrm{Box} - \frac{1}{2}\mathrm{Re}\left(\Sigma_L^e(0) + \Sigma_L^\mu(0) + \Sigma_L^{\nu_e}(0) + \Sigma_L^{\nu_\mu}(0)\right),\end{aligned} \tag{13}$$

with the photon vacuum polarization

$$\Pi^{AA}(k^2) = \frac{\Sigma_T^{AA}(k^2)}{k^2}. \tag{14}$$

Here Σ_L denotes the left-handed part of a fermion self-energy.

The contributions to Δr in the MSSM, besides the ones of SM type, consist of a large number of additional self-energy, vertex and box diagrams containing sfermions, (SUSY) Higgs bosons, charginos and neutralinos in the loop, see also Ref. [17]. In order to determine the contribution to Δr from a particular loop diagram, the Born amplitude has to be factored out of the one-loop muon decay amplitude, as shown in Eq. (10). While most loop diagrams directly give a result proportional to the Born amplitude, more complicated spinor structures that do not occur in the SM case arise from box diagrams containing neutralinos and charginos. Those spinor chains can be related to the Born amplitude with the help of Fierz identities and charge conjugation relations. The reduction of the box diagrams to Born-type amplitudes leads to coefficients containing ratios of mass-squared differences of the involved particles. These coefficients can give rise to numerical instabilities in cases of mass degeneracies. In the implementation of our results (which has been carried out in a `Mathematica` and a `Fortran` version) special care has been taken of such parameter regions with mass degeneracies or possible threshold effects, so that a numerically stable evaluation is ensured.

At the one-loop level, the quantity Δr can be split into three parts

$$\Delta r^{(\alpha)} = \Delta\alpha - \frac{c_\mathrm{w}^2}{s_\mathrm{w}^2}\Delta\rho + \Delta r_\mathrm{rem}. \tag{15}$$

The shift of the fine structure constant $\Delta\alpha$ arises from the charge renormalization which contains the contributions from light fermions. The quantity $\Delta\rho$ contains loop corrections to the ρ parameter [98], which describes the ratio between neutral and charged weak currents, and can be written as

$$\Delta\rho = \frac{\Sigma_T^{ZZ}(0)}{M_Z^2} - \frac{\Sigma_T^{WW}(0)}{M_W^2}\ . \tag{16}$$

predictions for Δr discussed in this paper internally make use of a definition of the gauge boson masses in terms of a Breit–Wigner shape with a fixed width. The values of the W and Z boson masses according to this fixed-width definition are finally converted into the running-width definition which has been adopted for the determination of the experimental values of M_W and M_Z, see e.g. Ref. [52] for further details.

[4]We adopt here the sign conventions for the covariant derivative used in `FeynArts` [91–96], which are different for the SM and the MSSM. Accordingly, sgn (the sign of the term involving the SU(2) coupling in the covariant derivative) in Eq. (13) for this choice of convention is sgn $= -1$ in the SM and sgn $= +1$ in the MSSM. Eq. (13) agrees with the corresponding formula given in Ref. [17] up to typographical errors in Ref. [17].

This quantity is sensitive to the mass splitting between the isospin partners in a doublet [98], which leads to a sizable effect in the SM in particular from the heavy fermion doublet. While $\Delta\alpha$ is a pure SM contribution, $\Delta\rho$ can get large contributions also from SUSY particles, in particular the superpartners of the heavy quarks. All other terms, both of SM and SUSY type, are contained in the remainder term $\Delta r_{\rm rem}$.

4.2 Incorporation of higher order corrections

The one-loop result described above has been combined with all available higher-order corrections. Since the calculation of Δr in the SM is more advanced than in the MSSM we have organized our result such that the full SM result for Δr can be used also for the MSSM prediction of M_W. Therefore the MSSM result is split into a SM part and a SUSY part[5]

$$\Delta r^{\rm MSSM} = \Delta r^{\rm SM} + \Delta r^{\rm SUSY} \,. \tag{17}$$

Writing the MSSM result in terms of Eq. (17) ensures in particular that in the decoupling limit of the MSSM result, where all superpartners are heavy and the Higgs sector becomes SM-like, the full SM result (with $M_H^{\rm SM} = M_h$) is recovered, see also the discussion in Ref. [17]. The SM part of Δr up to four-loop order is given by

$$\begin{aligned}\Delta r^{\rm SM} =& \Delta r^{(\alpha)} + \Delta r^{(\alpha\alpha_s)} + \Delta r^{(\alpha\alpha_s^2)} + \Delta r^{(\alpha^2)}_{\rm ferm} + \Delta r^{(\alpha^2)}_{\rm bos} \\ &+ \Delta r^{(G_\mu^2\alpha_s m_t^4)} + \Delta r^{(G_\mu^3 m_t^6)} + \Delta r^{(G_\mu m_t^2 \alpha_s^3)} \,.\end{aligned} \tag{18}$$

It contains, besides the one-loop contribution $\Delta r^{(\alpha)}$,

- the two-loop QCD corrections $\Delta r^{\alpha\alpha_s}$ [54–59],
- the three-loop QCD corrections $\Delta r^{\alpha\alpha_s^2}$ [65–68],
- the fermionic electroweak two-loop corrections $\Delta r^{(\alpha^2)}_{\rm ferm}$ [52, 60, 61],
- the purely bosonic electroweak two-loop corrections $\Delta r^{(\alpha^2)}_{\rm bos}$ [62–64],
- the mixed QCD and electroweak three-loop contributions $\Delta r^{G_\mu^2\alpha_s m_t^4}$ [69, 72],
- the purely electroweak three-loop contribution $\Delta r^{G_\mu^3 m_t^6}$ [69, 72],
- and the four-loop QCD correction $\Delta r^{(G_\mu m_t^2\alpha_s^3)}$ [71].

The full result for the electroweak two-loop contributions in the SM involves numerical integrations of the two-loop scalar integrals, which make the corresponding code rather unwieldy and slow. Thus, we make use of the simple parametrisation that has been given in Ref. [22] for the combined result of the fermionic and bosonic electroweak two-loop corrections in the SM, which approximates the exact result for $\Delta r^{(\alpha^2)}_{\rm ferm} + \Delta r^{(\alpha^2)}_{\rm bos}$ to better than 2.7×10^{-5}

[5] Since the complete one-loop results for Δr in the SM and in the MSSM are used in Eq. (17), this splitting has an impact only from the two-loop level onwards.

for 10 GeV $\leq M_H^{\rm SM} \leq$ 1 TeV (and the other input parameters in their $2\,\sigma$ ranges), corresponding to an uncertainty of 0.4 MeV for M_W. The use of a parametrisation directly for the SM prediction of $\Delta r_{\rm ferm}^{(\alpha^2)} + \Delta r_{\rm bos}^{(\alpha^2)}$ rather than for the full SM prediction of M_W leads to an improved accuracy in the combination with the SUSY contributions as compared to Ref. [17]. Concerning the QCD corrections, which enter from the two-loop level onwards, it should be noted that they result in a rather large (downward) shift of the W boson mass prediction. It is obvious that this kind of corrections needs to be theoretically well under control in order to gain sensitivity to effects of physics beyond the SM.

The quantity $\Delta r^{\rm SUSY}$ in Eq. (17) denotes the difference between Δr in the MSSM and the SM, i.e. it only involves the contributions from the additional SUSY particles and the extended Higgs sector. Beyond one-loop order, all SUSY corrections that are known to date are implemented, namely the leading reducible $\mathcal{O}(\alpha^2)$ two-loop corrections that can be obtained via the resummation formula given in Ref. [99], the leading SUSY two-loop QCD corrections of $\mathcal{O}(\alpha\alpha_s)$ to $\Delta\rho$ as given in Refs. [86, 87], as well as the dominant Yukawa-enhanced electroweak corrections of $\mathcal{O}(\alpha_t^2)$, $\mathcal{O}(\alpha_t\alpha_b)$, $\mathcal{O}(\alpha_b^2)$ to $\Delta\rho$ [88, 89]. In order to incorporate the latter corrections, the dominant Yukawa-enhanced electroweak corrections in the SM [100, 101] have been subtracted from the MSSM result presented in Ref. [89] according to Eq. (17). For this purpose we have identified the SM Higgs mass entering the result of Refs. [100, 101] with the mass of the MSSM Higgs boson that has the largest coupling to gauge bosons (i.e., the MSSM Higgs boson that behaves most SM-like). In the decoupling limit, where $M_A \gg M_Z$ and all superpartners are heavy, the MSSM contribution reduces to the SM contribution with $M_H^{\rm SM} = M_h$, so that the contribution to $\Delta r^{\rm SUSY}$ vanishes as required.

5 Numerical analysis

Our numerical results are based on the contributions to Δr described in the previous section (which have been implemented in a `Mathematica` and a `Fortran` version, where the latter has been used to generate the results presented below). The numerical values for the masses and effective couplings of the MSSM Higgs bosons have been evaluated with the help of the program `FeynHiggs` (version 2.9.4) [102–106]. We cross-checked our evaluation with the earlier results given in Ref. [17] and found good agreement, at the level of about 1–2 MeV.

5.1 Prediction for M_W in the SM

The mass of the signal discovered in the Higgs boson searches at the LHC about a year ago is measured mainly in the $\gamma\gamma$ and the $ZZ^{(*)}$ channels. Currently, the combined mass measurement from ATLAS is $125.5 \pm 0.2 \pm 0.6$ GeV [107] and from CMS $125.7 \pm 0.3 \pm 0.3$ GeV [108]. Adding systematic and statistical errors in quadrature and determining the weighted average between the ATLAS and CMS measurements we get $M_H^{\rm SM} = 125.64 \pm 0.35$ GeV. Setting the SM Higgs boson mass to this value, the SM prediction for the W boson mass reads (the other SM parameters have been fixed as $G_\mu = 1.1663787 \times 10^{-5}$, $M_Z = 91.1875$ GeV, $\alpha_s(M_Z) = 0.1180$, $\Delta\alpha_{\rm had} = 0.02757$)

$$M_W^{\rm SM}(m_t = 173.2\ {\rm GeV}, M_H^{\rm SM} = 125.64\ {\rm GeV}) = 80.361\ {\rm GeV}. \tag{19}$$

Accordingly, the SM prediction for M_W turns out to be below the current experimental value, $M_W^{\rm exp} = 80.385 \pm 0.015$ GeV, by about $1.5\,\sigma$. The dominant theoretical uncertainty of the prediction for M_W arises from the parametric uncertainty induced by the experimental error in the measurement of the top-quark mass. An experimental error of 1 GeV on m_t causes a parametric uncertainty on M_W of about 6 MeV, while the parametric uncertainties induced by the current experimental error of the hadronic contribution to the shift in the fine-structure constant, $\Delta\alpha_{\rm had}$, and by the experimental error of M_Z amount to about 2 MeV and 2.5 MeV, respectively. The uncertainty of the M_W prediction caused by the experimental error of the Higgs mass $\delta M_H^{\rm exp} = 0.35$ GeV is significantly smaller (~ 0.2 MeV). The uncertainties from unknown higher-order corrections have been estimated to be around 4 MeV in the SM for a light Higgs boson ($M_H^{\rm SM} < 300$ GeV) [74].

5.2 MSSM parameter scan: Scan ranges and constraints

The prediction for M_W in the MSSM is affected by additional theoretical uncertainties from unknown higher-order corrections of SUSY type. While in the decoupling limit those additional uncertainties vanish, they can be important if some SUSY particles, in particular in the scalar top and bottom sectors, are relatively light. The combined theoretical uncertainty from unknown higher-order corrections of SM- and SUSY-type has been estimated (for the MSSM with real parameters) in Refs. [17, 89] as $\delta M_W = (4.7 - 9.4)$ MeV, depending on the SUSY mass scale.

In the following we will investigate the prediction for M_W in the MSSM based on scans of the MSSM parameters over a wide range (using flat distributions). We have performed two versions of those random scans, one where the top-quark mass is kept fixed at $m_t = 173.2$ GeV and one where also m_t is allowed to vary in the scan. Both scans use initially $\sim 5 \times 10^6$ points, and dedicated smaller scans have been performed in parameter regions where the SUSY contributions to M_W are relatively large. The scan ranges are given in Table 1. We have assumed that the value of M_1 is fixed by the one of M_2 in terms of the usual GUT relation, $M_1 = 5/3\, s_{\rm w}^2/c_{\rm w}^2\, M_2$. As mentioned above, we restrict our numerical analysis to the case of real parameters. We include CKM mixing, but the numerical effect turns out to be negligible (below 0.01 MeV in M_W). Possible flavor violation in the SUSY sector [19] is neglected here. In order to avoid unphysical parameter regions and regions of numerical instabilities we disregard parameter points for which `FeynHiggs` indicates a large theoretical uncertainty in the evaluation of the Higgs mass predictions. We furthermore exclude points where stop and sbottom masses are mass-degenerate within less than 0.1 GeV causing numerical instabilities in the gluino corrections of $\mathcal{O}(\alpha\alpha_s)$ to $\Delta\rho$.

All MSSM points included in our results have the lightest neutralino as LSP and have SUSY particle masses that pass the lower mass limits from direct searches at LEP. The Higgs and SUSY masses are calculated from the MSSM input parameters using `FeynHiggs` (version 2.9.4) [103–106]. In the SM and SUSY higher-order corrections, as listed in Sect. 4.2, the bottom-quark mass has been renormalized in the on-shell scheme. Accordingly, in our evaluation of M_W the bottom-quark pole mass, $m_b^{\rm pole}$, is used everywhere. This also applies to the calculation of the sbottom masses from the MSSM input parameters, and we have modified the corresponding routine in `FeynHiggs` accordingly (in the calculation of the sbottom masses furthermore a Δ_b [109–112] correction enters, which can be absorbed into an

Parameter	Minimum	Maximum
μ	-2000	2000
$M_{\tilde{E}_{1,2,3}} = M_{\tilde{L}_{1,2,3}}$	100	2000
$M_{\tilde{Q}_{1,2}} = M_{\tilde{U}_{1,2}} = M_{\tilde{D}_{1,2}}$	500	2000
$M_{\tilde{Q}_3}$	100	2000
$M_{\tilde{U}_3}$	100	2000
$M_{\tilde{D}_3}$	100	2000
$A_e = A_\mu = A_\tau$	$-3\, M_{\tilde{E}}$	$3\, M_{\tilde{E}}$
$A_u = A_d = A_c = A_s$	$-3\, M_{\tilde{Q}_{12}}$	$3\, M_{\tilde{Q}_{12}}$
A_b	$-3 \max(M_{\tilde{Q}_3}, M_{\tilde{D}_3})$	$3 \max(M_{\tilde{Q}_3}, M_{\tilde{D}_3})$
A_t	$-3 \max(M_{\tilde{Q}_3}, M_{\tilde{U}_3})$	$3 \max(M_{\tilde{Q}_3}, M_{\tilde{U}_3})$
$\tan\beta$	1	60
M_3	500	2000
M_A	90	1000
M_2	100	1000

Table 1: Parameter ranges considered in the scans. All parameters with mass dimension are given in GeV.

effective bottom-quark mass). For every parameter point we test whether it is allowed by direct Higgs searches using the code `HiggsBounds` (version 4.0.0) [40–42]. This code tests the compatibility of the MSSM points with the search limits from LEP, the Tevatron and the LHC. Running `HiggsBounds`, we take into account the theoretical uncertainties on the Higgs masses using the estimate provided by `FeynHiggs`.

Our results presented below improve on earlier results given in Ref. [17] in several respects. We study here the impact of both the limits from the Higgs boson searches as well as from the signal observed at about 125.6 GeV. Furthermore we investigate constraints from present and possible future limits from searches for SUSY particles. On a more technical level, our analysis incorporates the SUSY two-loop corrections of $\mathcal{O}(\alpha_t^2)$, $\mathcal{O}(\alpha_t\alpha_b)$, $\mathcal{O}(\alpha_b^2)$, which were not included in the scan results presented previously, and we perform a more detailed scan involving a larger number of sampling points.

5.3 Results for M_W in the MSSM

In this section we study the MSSM prediction for M_W, starting in Fig. 1 where M_W is displayed as a function of the top-quark mass, m_t, in the SM and the MSSM. The green area shows the MSSM parameter space that is allowed by `HiggsBounds` and the various other constraints described in the previous subsection. It should be noted that in this plot only the limits from the Higgs searches are considered as constraints on the MSSM parameter space, not the observed signal at about 125.6 GeV (the latter will be discussed below). The region where the MSSM prediction for M_W overlaps with the one in the SM is indicated by the red strip, where $M_H^{\rm SM} = 125.6 \pm 0.7$ GeV (corresponding roughly to the $2\,\sigma$ experimental error on M_H) has been used for the SM prediction. The left plot shows the results on a larger scale, in order to indicate the possible range of the MSSM prediction, while the right plot is a zoom into the parameter region of the MSSM near the experimental central values of M_W

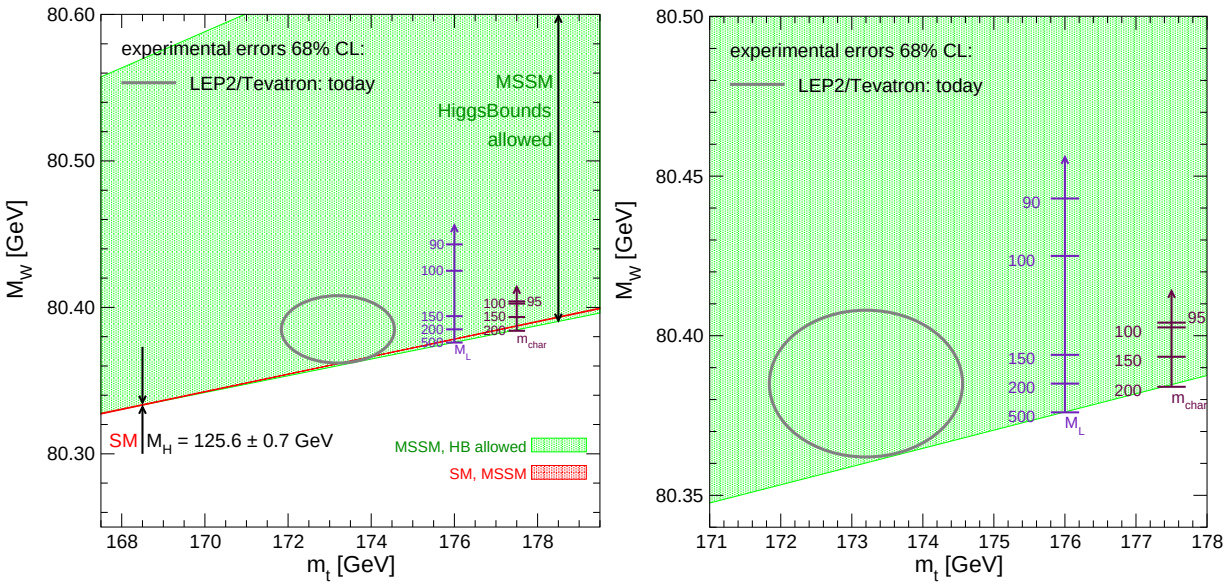


Figure 1: Prediction for M_W as a function of m_t. Left: The green region shows the `HiggsBounds` allowed region for the MSSM M_W prediction. It has been obtained by scanning over the MSSM parameters as described in the text. The cuts $m_{\tilde{t}_2}/m_{\tilde{t}_1} < 2.5$ and $m_{\tilde{b}_2}/m_{\tilde{b}_1} < 2.5$ are applied. The red strip indicates the overlap region of the SM and the MSSM, with $M_H^{\rm SM} = 125.6 \pm 0.7$ GeV. The two arrows indicate the possible size of the slepton and the chargino (and neutralino) contributions. Right: zoom into the most relevant region, with the SM area omitted.

and m_t. In order to obtain the MSSM prediction shown as the green band in Fig. 1 we have imposed as an additional restriction a limit on the mass splittings in the stop and sbottom sector, which has been implemented via the conditions $m_{\tilde{t}_2}/m_{\tilde{t}_1} < 2.5$ and $m_{\tilde{b}_2}/m_{\tilde{b}_1} < 2.5$. If no such condition on the mass splittings in the stop and sbottom sector were imposed, even larger values of M_W (up to ~ 80.8 GeV) would be possible in the MSSM, see also the discussion in Ref. [17]. Since this parameter region far above the experimental value of M_W is of little phenomenological interest, we will not consider it further here. While it is well-known that a non-zero SUSY contribution tends to increase the prediction for M_W as compared to the SM case, close inspection of Fig. 1 reveals that there exists a small MSSM (green) region below the overlap region between the MSSM and the SM (red), which is best visible for the largest m_t values. The reason for this feature lies in the fact that, as explained above, the SM prediction is shown for the range $M_H^{\rm SM} = 125.6 \pm 0.7$ GeV, while no restriction from the signal observed in the Higgs searches has been applied to the MSSM parameter space. As a consequence, the MSSM region (green) contains parameter points where the lightest $\mathcal{CP}$-even Higgs boson of the MSSM has a mass above the range allowed for $M_H^{\rm SM}$ (and below the upper bound on M_h in the MSSM, which increases with increasing m_t). In the decoupling region, where all superpartners are heavy, the MSSM prediction for M_W in this case corresponds to the prediction in the SM with a higher value of $M_H^{\rm SM}$, which yields

a lower value of M_W[6].

The predictions for M_W in the SM and the MSSM are compared with the current experimental results for M_W and m_t [6] which are displayed by the corresponding 68% C.L. ellipse shown in gray. One can see that the SM prediction barely touches the 68% C.L. ellipse, whereas the ellipse is fully contained in the MSSM area. It is obvious that the MSSM contains parameter regions where the MSSM prediction for M_W is in very good agreement with the data. On the other hand, also M_W values significantly above the experimental value are possible in the MSSM. The latter arise mainly from very light states and a large mass splitting in the stop and sbottom sector (see the discussion below).

Fig. 1 shows that confronting the prediction for M_W in the MSSM with the experimental result is of interest both for putting constraints on parameter regions that would give rise to a too high value of M_W and for investigating the parameter region where the agreement between the MSSM prediction and the data is in fact better than for the SM case. While the deviation between the SM prediction and the experimental result for M_W is statistically not very significant (the SM prediction is well compatible with the experimental result at the 95% C.L.), the pattern that the SM prediction is somewhat low as compared to the data has been robust for many years in spite of numerous updates of the experimental results. Focussing now on the region where we find the best agreement between the MSSM prediction for M_W and the experimental result, it is interesting to note that in this region some of the superpartner masses are expected to be relatively light. In order to illustrate this feature we furthermore show in Fig. 1 the impact of the slepton sector (left arrow) and the chargino sector (right arrow), where the mass values indicated at the arrows (approximately) show the effect in M_W arising from the contribution of a slepton and a chargino having this mass, respectively. We have chosen to display those arrows such that they start at the lower border, corresponding to the situation where all other superpartners are heavy and decoupled. For the sleptons we show the corrections to M_W as a function of $M_L \equiv M_{\tilde{E}_{1,2,3}} = M_{\tilde{L}_{1,2,3}}$, where the lower limit of ~ 90 GeV roughly corresponds to the (fairly model-independent) limit obtained at LEP. One can see that very light sleptons, just above the LEP limit, could induce a shift in M_W of about 60 MeV. We have checked that each generation contributes roughly the same to this effect. The major contributions to M_W from the sleptons arise from the $\Delta\rho$ term in Eq. (15), which is sensitive to the mass splitting between $\tilde{l}_{1,2}$ and $\tilde{\nu}_l$. The splitting between the sneutrinos and the sleptons becomes significant if $M_{\tilde{E}} = M_{\tilde{L}}$ and M_W are of comparable size. The contributions to M_W from light charginos and neutralinos are substantially smaller, but clearly not negligible in this context. They reach about 20 MeV for $m_{\tilde{\chi}_1^\pm} \sim 95$ GeV, close to its lower mass limit from LEP. In that case, due to the assumed GUT relation between M_1 and M_2, the mass of $\tilde{\chi}_1^0$ is ~ 50 GeV. Our analysis of the contributions in the slepton and the chargino / neutralino sector shows that even if all squarks were so heavy that their contribution to the M_W prediction were negligible, contributions from the slepton sector or the chargino / neutralino sector could nevertheless be sufficient to bring the MSSM prediction in perfect agreement with the data. This could be the case for slepton

[6]It should be noted that a similar kind of feature would occur even if one restricted the predicted value for M_h in the MSSM to the same region as the range adopted for $M_H^{\rm SM}$. This is caused by the fact that the additional theoretical uncertainties from unknown higher-order corrections affecting the prediction for M_h in the MSSM, which are not present in the SM where $M_H^{\rm SM}$ is a free input parameter, essentially lead to a broadening of the allowed range of M_h in the MSSM as compared to $M_H^{\rm SM}$.

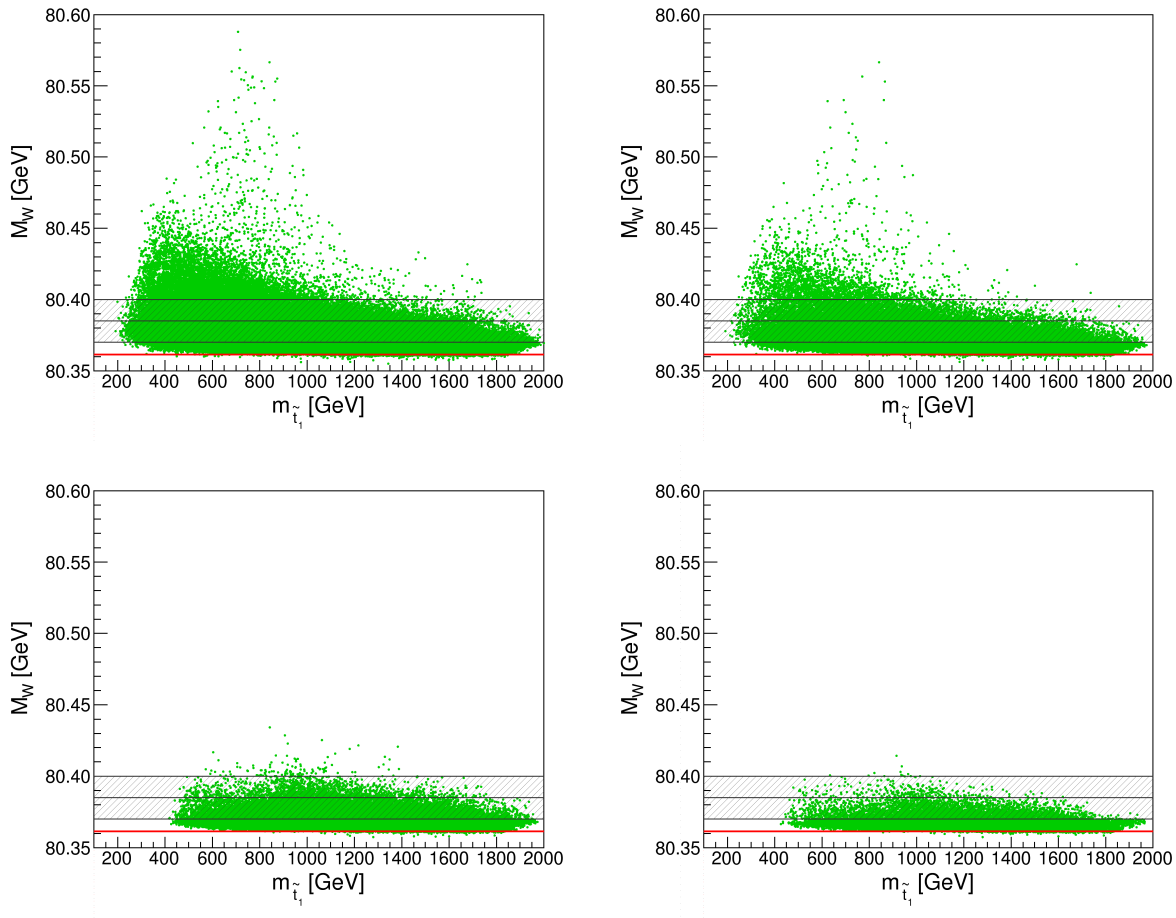


Figure 2: Prediction for M_W as a function of the lightest stop mass $m_{\tilde{t}_1}$. In all plots the cuts $m_{\tilde{t}_2}/m_{\tilde{t}_1} < 2.5$ and $m_{\tilde{b}_2}/m_{\tilde{b}_1} < 2.5$ are applied. In the upper left plot all `HiggsBounds` allowed points are shown, in the upper right plot only the points are shown for which additionally the squarks of the first two generations and the gluino are heavier than 1200 GeV, in the lower left plot only the points are shown for which additionally the sbottoms are heavier than 1000 GeV, and in the lower right plot only the points are shown for which additionally also the sleptons and charginos are heavier than 500 GeV. The red line indicates the SM prediction for M_W.

masses of about 150–200 GeV or for a chargino mass of about 100–150 GeV. If the squark sector gives rise to a non-zero contribution to M_W the same predicted value for M_W could be reached with heavier sleptons and charginos / neutralinos.

In Fig. 2 and Fig. 3 we analyze in detail the dependence of M_W on the scalar quark masses, in particular on $m_{\tilde{t}_1}$ and $m_{\tilde{b}_1}$, with m_t fixed to 173.2 GeV. The upper left plot of Fig. 2 shows the prediction for M_W (green dots) as a function of $m_{\tilde{t}_1}$. All points are allowed by the constraints discussed in Sect. 5.2 and fulfill the additional constraint $m_{\tilde{t}_2,\tilde{b}_2}/m_{\tilde{t}_1,\tilde{b}_1} < 2.5$. The SM prediction is shown as a red strip for $M_H^{\rm SM} = 125.6 \pm 0.7$ GeV, and the $1\,\sigma$ experimental result is indicated as a gray dashed band. We checked that without the cut $m_{\tilde{t}_2,\tilde{b}_2}/m_{\tilde{t}_1,\tilde{b}_1} < 2.5$ the largest M_W values are reached for very light stop masses with a very

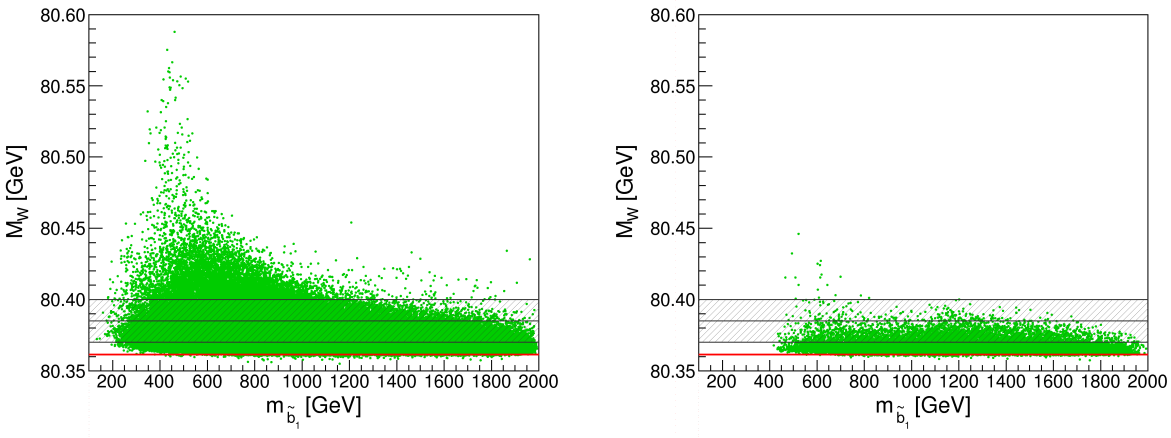


Figure 3: Prediction for M_W as a function of the lightest sbottom mass. The cuts $m_{\tilde{t}_2}/m_{\tilde{t}_1} < 2.5$ and $m_{\tilde{b}_2}/m_{\tilde{b}_1} < 2.5$ are applied. In the left plot all `HiggsBounds` allowed points are shown, in the right plot only the points are shown for which additionally the squarks of the first two generations and the gluino are heavier than 1200 GeV, stops are heavier than 1000 GeV and also the sleptons and charginos are heavier than 500 GeV. As above, the red line indicates the SM prediction for M_W.

large (> 2.5) splitting in the stop sector. Now the maximum of ~ 80.6 GeV is reached for $m_{\tilde{t}_1}$ around 800 GeV. The position where the maximum is reached depends strongly on the splitting between stops and sbottoms and will be further explained below (in the discussion of Fig. 3). In the upper right plot we only show points which have first and second generation squark masses and the gluino mass above 1.2 TeV, i.e. roughly at the limit obtained at the LHC for simplified spectra [25–28]. It can be observed that the effects on M_W of the first and second generation squarks as well as of the gluino are rather mild. Next, in the lower left plot we only show points which in addition have $\tilde{b}$ masses above 1000 GeV (this is a hypothetical cut that is applied for illustration purposes only; it does not reflect the current experimental situation). The fact that all MSSM points in the lower left and lower right plots have stop masses larger than 400 GeV results from the restrictions that we have imposed, constraining the sbottom masses (> 1000 GeV) and the maximal splitting in the stop and sbottom sector ($m_{\tilde{t}_2,\tilde{b}_2}/m_{\tilde{t}_1,\tilde{b}_1} < 2.5$) at the same time. Clearly the sbottoms have a large impact on the M_W prediction. After applying (for illustration) the sbottom mass cut the maximal M_W values obtained in the scan are ~ 80.43 GeV, i.e. the SUSY contributions can still be so large in this case that they can yield not only predicted M_W values that are in good agreement with the experimental result but also ones that are significantly higher. The SUSY shift in this case is caused by the remaining contribution from the stop–sbottom sector, as well as by the contributions from charginos, neutralinos and sleptons. In order to disentangle these effects, in the lower right plot we also require (again, for illustrative purposes only) the electroweak SUSY particles to be heavy and show only points with slepton and chargino masses above 500 GeV. A direct mass limit on neutralinos is not applied. Since we fixed $M_1 \approx \frac{1}{2}M_2$, all points have neutralino masses above ~ 240 GeV. In this plot the shift in the M_W prediction as compared to the SM case arises solely from the stop–sbottom sector with $m_{\tilde{b}_1} > 1000$ GeV

(neglecting the numerically insignificant contributions from the other sectors for large SUSY particle masses). One can observe that M_W values up to the upper edge of the experimental $1\,\sigma$ band (~ 80.400 GeV) can still be reached for $m_{\tilde{t}_1}$ values as high as $m_{\tilde{t}_1} \sim 1100$ GeV in this case. For large stop masses, $m_{\tilde{t}_1} \gtrsim 1100$ GeV, the contributions from the stop–sbottom sector decrease as expected in the decoupling limit.[7]

Now we turn to Fig. 3 showing the M_W prediction plotted against $m_{\tilde{b}_1}$. In the left plot we show all points that are allowed by `HiggsBounds` and the other constraints described above (in particular, $m_{\tilde{t}_2}/m_{\tilde{t}_1} < 2.5$ and $m_{\tilde{b}_2}/m_{\tilde{b}_1} < 2.5$ is required). In the right plot only those points are displayed for which the stops are heavier than 1000 GeV, the first and second generation squark masses as well as the gluino mass are above 1200 GeV, and the sleptons and charginos are heavier than 500 GeV. Focusing first on the left plot, one can see that it displays the same qualitative features as the upper left plot of Fig. 2. While one would normally expect that the highest values for M_W are obtained for the smallest values of $m_{\tilde{t}_1}$ and $m_{\tilde{b}_1}$, in the corresponding plots of Fig. 2 and Fig. 3 the highest M_W values are found for $m_{\tilde{t}_1} \sim 800$ GeV and $m_{\tilde{b}_1} \sim 400$ GeV. This feature is related to the imposed restriction that the maximal mass splitting for stop and sbottom masses is limited to be smaller than 2.5. The largest correction to M_W originates from the stop–sbottom contributions to $\Delta\rho$, which depend sensitively on the mass splittings between the four squarks of the third generation. After imposing the limit on the maximal mass splittings of stops and sbottoms, these contributions become largest if the relative size of the sbottom mixing, $|X_b/\max(M_{\tilde{Q}_3}, M_{\tilde{D}_3})|$, reaches its maximum. This is realized in this case for $m_{\tilde{b}_1} \sim 400$ GeV and $m_{\tilde{b}_2}/m_{\tilde{b}_1} \sim 2.5$, $m_{\tilde{t}_1}/m_{\tilde{b}_1} \sim 2$, giving rise to the maximum around $m_{\tilde{t}_1} \sim 800$ GeV and $m_{\tilde{b}_1} \sim 400$ GeV in the upper left plot of Fig. 2 and the left plot of Fig. 3, respectively. As expected, for higher values of $m_{\tilde{b}_1}$ the maximum value reached for M_W in Fig. 3 decreases, but M_W values as high as the experimental central value are seen to be possible all the way up to $m_{\tilde{b}_1} \sim 2$ TeV. In the right plot the other SUSY particles are required to be rather heavy (in particular, the stop masses are assumed to be above 1000 GeV; the other masses are restricted as described above), so that the impact of the contributions from the sbottom sector becomes apparent. While rather large contributions are possible for sbottom masses below about 800 GeV, for the highest values of $m_{\tilde{b}_1}$ shown in the figure the MSSM prediction for M_W approaches the one in the SM.

So far we have only taken into account the existing *limits* from the Higgs searches at the LHC and other colliders (via the program `HiggsBounds`), but we have not explicitly imposed a constraint in view of the observed *signal* at ~ 125.6 GeV. Within the MSSM (referring to the $\mathcal{CP}$-conserving case for simplicity), the signal can, at least in principle, be identified either with the light $\mathcal{CP}$-even Higgs boson h or the heavy $\mathcal{CP}$-even Higgs boson H. In Fig. 4 we show the SM and MSSM prediction of M_W as a function of m_t as obtained from our scan according to Table 1, where in the left plot the green MSSM area fulfills $M_h = 125.6 \pm 3.1$ GeV, while in the right plot the green MSSM area fulfills $M_H = 125.6 \pm 3.1$ GeV. The substantially larger uncertainty with respect to the SM experimental uncertainty of 0.7 GeV (at the $2\,\sigma$ level) arises as a consequence of the theoretical uncertainties from unknown higher-order

[7] In all plots in Fig. 2 one can see a small gap between the MSSM points for $m_{\tilde{t}_1} > 1900$ GeV and the SM line. This is an artefact of the chosen scan ranges: in this region the mass-splitting between $\tilde{t}_1$ and $\tilde{t}_2$ is small, and m_h does not reach values up to ~ 126 GeV. The M_W value approached in the decoupling limit therefore corresponds to the SM prediction for a lower Higgs mass value.

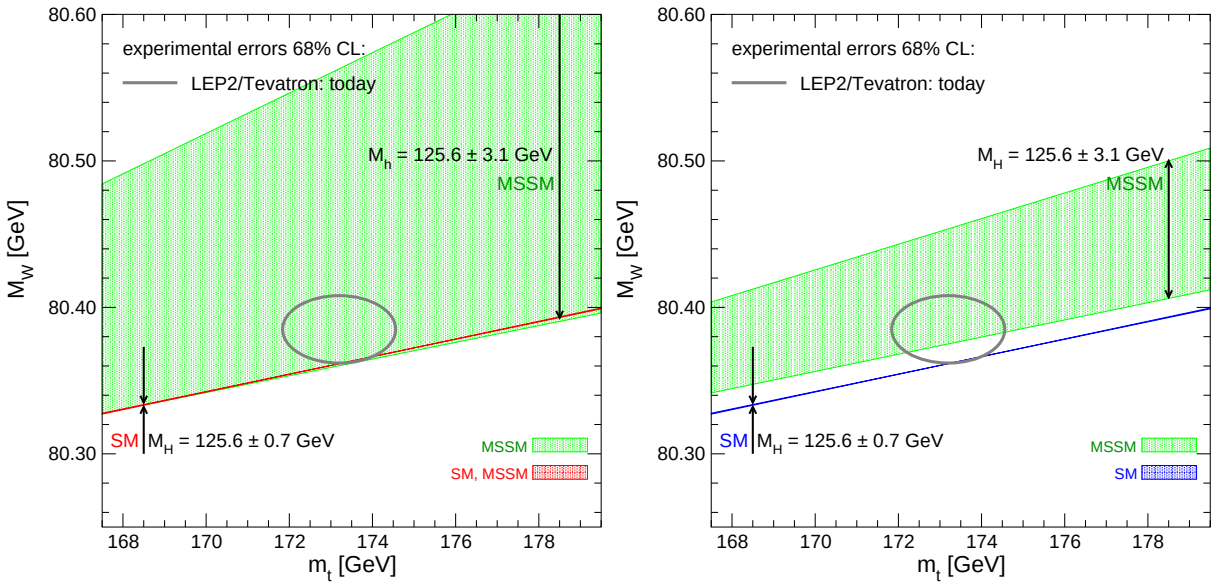


Figure 4: Prediction for M_W as a function of m_t. The left plot shows the M_W prediction assuming the *light* $\mathcal{CP}$-even Higgs boson h in the mass region 125.6 ± 3.1 GeV. The red band indicates the overlap region of the SM and the MSSM with $M_H^{\rm SM} = 125.6 \pm 0.7$ GeV. The right plot shows the M_W prediction assuming the *heavy* $\mathcal{CP}$-even Higgs boson H in the mass region 125.6 ± 3.1 GeV. The blue band again indicates the SM region with $M_H^{\rm SM} = 125.6 \pm 0.7$ GeV. All points are allowed by `HiggsBounds`.

corrections in the MSSM prediction for the Higgs boson mass. We have added a global uncertainty of 3 GeV [104] in quadrature, yielding a total uncertainty of 3.1 GeV.

Starting with the left plot, where the light $\mathcal{CP}$-even Higgs boson has a mass that is compatible with the observed signal, we find a similar result as in Fig. 1. In particular, the comparison with the experimental results for M_W and m_t, indicated by the gray ellipse, shows a slight preference for a non-zero SUSY contribution to M_W. While the width of the MSSM area shown in green is somewhat reduced compared to Fig. 1 because of the additional constraint applied here (requiring M_h to be in the range $M_h = 125.6 \pm 3.1$ GeV leads to a constraint on the stop sector parameters, see, e.g., Ref. [32], which in turn limits the maximal contribution to M_W), the qualitative features are the same as in Fig. 1. This is not surprising, since the limits from the Higgs searches implemented in Fig. 1 have already led to a restriction of the allowed mass range to the unexcluded region near the observed signal. As in Fig. 1 the plot shows a small MSSM region (green) below the overlap region between the MSSM and the SM (red), which is a consequence of the broadening of the allowed range of M_h caused by the theoretical uncertainties from unknown higher-order corrections, as explained above.

In the right plot of Fig. 4 we show the result for the case where instead the mass of the heavy $\mathcal{CP}$-even Higgs boson is assumed to be compatible with the observed signal, i.e. $M_H = 125.6 \pm 3.1$ GeV. While as mentioned above the interpretation of the discovered signal in terms of the heavy $\mathcal{CP}$-even Higgs boson within the MSSM is challenged in particular by the recent ATLAS bound on light charged Higgs bosons [39] (which is not yet included in the

version of HiggsBounds used for our analysis),[8] it is nevertheless interesting to investigate to what extent the precision observable M_W is sensitive to such a rather exotic scenario where all five states of the MSSM Higgs sector are light. The lightest $\mathcal{CP}$-even Higgs in this scenario has a heavily suppressed coupling to gauge bosons and a mass that can be significantly below the LEP limit for a SM-like Higgs, see e.g. Ref. [33]. As shown in the right plot of Fig. 4, the constraint $M_H = 125.6 \pm 3.1$ GeV gives rise to a situation where the MSSM region (green) does not overlap with the SM prediction (blue). This gap between the predictions of the two models is caused by the fact that $M_H = 125.6 \pm 3.1$ GeV implies light states in the Higgs sector (in particular a light charged Higgs), which lead to a non-zero SUSY contribution to M_W in this case, whereas for the light $\mathcal{CP}$-even Higgs boson the constraint $M_h = 125.6 \pm 3.1$ GeV can be fulfilled in the decoupling region of the MSSM. The plot furthermore shows that the constraint $M_H = 125.6 \pm 3.1$ GeV implies not only a lower bound on the SUSY contribution to M_W but also a more restrictive upper bound, as can be seen from comparing the two plots in Fig. 4. It is interesting to note that also in the case where the heavy $\mathcal{CP}$-even Higgs is in the mass range compatible with the observed signal, the MSSM turns out to be better compatible with the experimental results for M_W and m_t (indicated by the gray ellipse) than the SM.

In Fig. 5 we analyze the dependence of the M_W prediction on light scalar taus. In Refs. [114, 115] it was shown that light scalar taus can enhance the decay rate of the light $\mathcal{CP}$-even Higgs boson into photons. This is of interest in view of the current experimental situation, where the signal strength in the $\gamma\gamma$ channel observed by ATLAS [116] lies significantly above the value expected in the SM (but is still compatible at the $2\,\sigma$ level), while the signal strength observed in CMS [117] is currently slightly below the SM level. Since loop contributions of BSM particles to the decay width $\Gamma(h \to \gamma\gamma)$ do not have to compete with a SM-type tree-level contribution, this loop-induced quantity is of particular relevance for investigating possible deviations from the SM prediction. Fig. 5 shows the prediction for M_W as a function of $\Gamma(h \to \gamma\gamma)/\Gamma(H \to \gamma\gamma)_{\rm SM}$, where the latter has been evaluated with FeynHiggs. As a starting point we use the best-fit point obtained in Ref. [34] from a pMSSM-7 fit to all Higgs data (available at that time), which indeed exhibited an enhancement of $\Gamma(h \to \gamma\gamma)$ due to scalar taus with a mass close to 100 GeV. The parameters of the best fit point are $M_A = 669$ GeV, $\tan\beta = 16.5$, $\mu = 2640$ GeV, $M_{\tilde{Q}_3} = M_{\tilde{U}_3} = M_{\tilde{D}_3} = 1100$ GeV, $M_{\tilde{Q}_{1,2}} = M_{\tilde{U}_{1,2}} = M_{\tilde{D}_{1,2}} = 1000$ GeV, $M_{\tilde{L}_3} = M_{\tilde{E}_3} = 285$ GeV, $M_{\tilde{L}_{1,2}} = M_{\tilde{E}_{1,2}} = 300$ GeV, $A_f = 2569$ GeV, $M_2 = 201$ GeV and $M_3 = 1000$ GeV. In Fig. 5 the best-fit point is indicated as a black star. We vary the stau mass scale $M_{\tilde{E}_3} = M_{\tilde{L}_3}$ in the range of 280 GeV to 500 GeV, giving rise to a corresponding variation of the lighter stau mass. The results are shown as the green line in Fig. 5, where the current experimental $1\,\sigma$ region for M_W is indicated as a gray band. One can observe that for light scalar taus, corresponding to larger $\Gamma(h \to \gamma\gamma)$, the agreement of the prediction for M_W with the experimental value is improved. A certain level of enhancement of $\Gamma(h \to \gamma\gamma)$ is also compatible with the current experimental results on the signal strength in the $\gamma\gamma$ channel. For heavy scalar taus, as obtained for $M_{\tilde{E}_3} = M_{\tilde{L}_3} = 500$ GeV (and keeping the other parameters as defined above), the M_W prediction still remains within the experimental $1\,\sigma$ band, while nearly SM values

[8] If the Higgs sector contains an additional singlet, as in the NMSSM, it is possible to have a SM-like second-lightest Higgs, while the charged Higgs boson can be much heavier in this case, see e.g. Ref. [113].

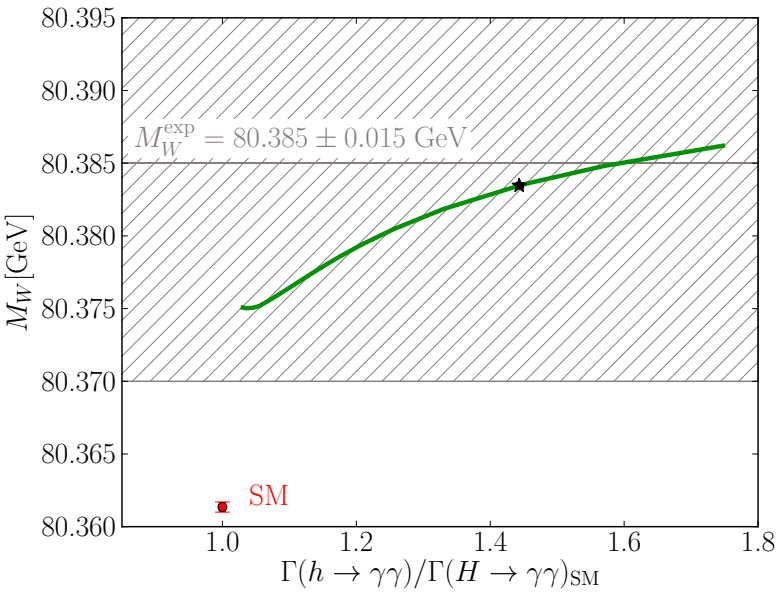


Figure 5: M_W prediction in the MSSM as a function of $\Gamma(h \to \gamma\gamma)$, normalized to the SM value. The black star indicates the best fit point from a pMSSM-7 fit to all Higgs data (available at that time) [34]. The green line is obtained by varying $M_{\tilde{E}_3} = M_{\tilde{L}_3}$ from 280 GeV to 500 GeV.

for $\Gamma(h \to \gamma\gamma)$ are reached.

5.4 Discussion of possible future scenarios

In the final step of our investigation we discuss the precision observable M_W in the context of possible *future* scenarios. We first investigate the impact of an assumed limit of 500 GeV on stops and sbottoms (and assume that no other colored particles are observed below 1200 GeV). In Fig. 6 we show again the M_W–m_t planes as presented in Fig. 1 (where the parameter region allowed by `HiggsBounds` is displayed) and in Fig. 4 (M_h or M_H in the range of 125.6 ± 3.1 GeV), but now in addition the light blue points obey the (hypothetical) mass limits for stops and sbottoms (500 GeV) and for other colored particles (1200 GeV). The left plot shows the `HiggsBounds` allowed points, whereas in the middle (right) plot $M_h(M_H) = 125.6 \pm 3.1$ GeV is required. It can be observed that the light blue points corresponding to a relatively heavy colored spectrum are found at the lower end of the predicted M_W range, i.e. in the decoupling region of the MSSM. As discussed above the largest SUSY contributions arise from the stop–sbottom sector. If lower lower mass limits on stops and sbottoms of 500 GeV are assumed, it can be seen that the band corresponding to the possible range of predictions for M_W in the MSSM would shrink significantly, to the region populated by the blue points. It should be noted that the prediction for M_W in this region is in perfect agreement with the experimental measurements of M_W and m_t. Besides the contributions of stops and sbottoms, which can still be significant even if the stops and sbottoms are heavier than 500 GeV, the main SUSY corrections arise from relatively light

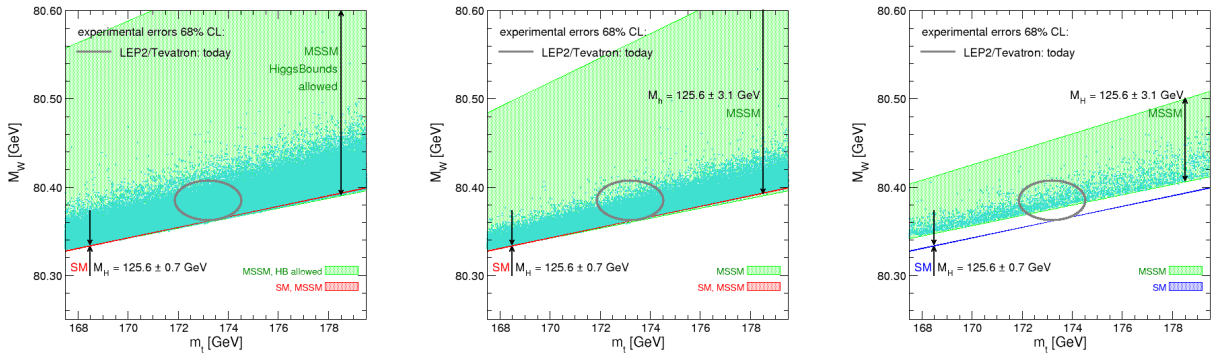


Figure 6: Prediction for M_W as a function of m_t. The left plot shows all points allowed by `HiggsBounds`, the middle one requires M_h to be in the mass region 125.6 ± 3.1 GeV, while in the right plot M_H is required to be in the mass region 125.6 ± 3.1 GeV. The color coding is as in Figs. 1 and 4. In addition, the blue points are the parameter points for which the stops and sbottoms are heavier than 500 GeV and squarks of the first two generations and the gluino are heavier than 1200 GeV.

sleptons, charginos and neutralinos, as analyzed above.

While so far we have compared the various predictions with the current experimental results for M_W and m_t, we now discuss the impact of future improvements of these measurements. For the W boson mass we assume an improvement of a factor three compared to the present case down to $\Delta M_W = 5$ MeV from future measurements at the LHC and a prospective Linear Collider (ILC) [118], while for m_t we adopt the anticipated ILC accuracy of $\Delta m_t = 100$ MeV [119]. For illustration we show in Fig. 7 again the left plot of Fig. 4, assuming the mass of the light $\mathcal{CP}$-even Higgs boson h in the region 125.6 ± 3.1 GeV, but supplement the gray ellipse indicating the present experimental results for M_W and m_t with the future projection indicated by the red ellipse (assuming the same experimental central values). While currently the experimental results for M_W and m_t are compatible with the predictions of both models (with a slight preference for a non-zero SUSY contribution), the anticipated future accuracies indicated by the red ellipse would clearly provide a high sensitivity for discriminating between the models and for constraining the parameter space of BSM scenarios.

As a further hypothetical future scenario we assume that a light scalar top quark has been discovered at the LHC with a mass of $m_{\tilde{t}_1} = 400 \pm 40$ GeV, while no other new particle has been observed. As before, for this analysis we use an anticipated experimental precision of $\Delta M_W = 5$ MeV (other uncertainties have been neglected in this analysis). Concerning the masses of the other SUSY particles, we assume lower limits of 300 GeV on both sleptons and charginos, 500 GeV on other scalar quarks of the third generation and of 1200 GeV on the remaining colored particles. We have selected the points from our

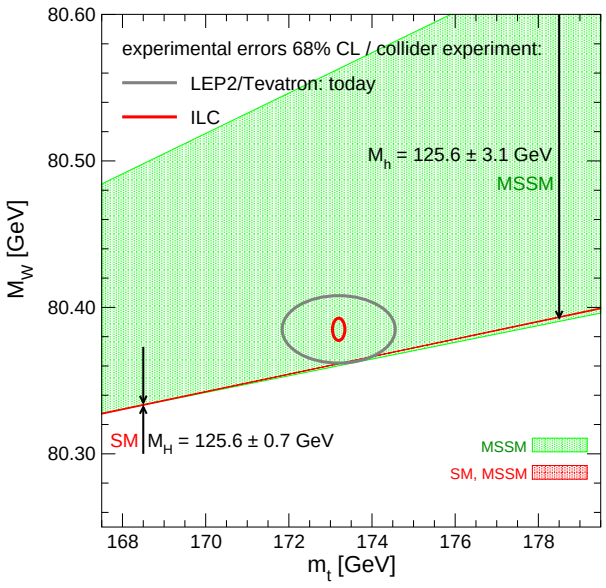


Figure 7: Prediction for M_W as a function of m_t, as given in the left plot of Fig. 4 (the mass M_h of the light $\mathcal{CP}$-even Higgs boson is assumed to be in the region 125.6 ± 3.1 GeV). In addition to the current experimental results for M_W and m_t that are displayed by the gray 68% C.L. ellipse the anticipated future precision at the ILC is indicated by the red ellipse (assuming the same experimental central values).

scan accordingly. Any additional particle observation would impose a further constraint and would thus enhance the sensitivity of the parameter determination. In Fig. 8 we show the parameter points from our scan that are compatible with the above constraints. All points fulfill $M_h = 125.6 \pm 3.1$ GeV and $m_{\tilde{t}_1} = 400 \pm 40$ GeV. Yellow, red and blue points have furthermore a W boson mass of $M_W = 80.375, 80.385, 80.395 \pm 0.005$ GeV, respectively, corresponding to three hypothetical future central experimental values for M_W. The left plot in Fig. 8 shows the M_W prediction as a function of the lighter sbottom mass. Assuming that the experimental central value for M_W stays at its current value of 80.385 GeV (red points) or goes up by 10 MeV (blue points), the precise measurement of M_W would set stringent upper limits of ~ 800 GeV (blue) or ~ 1000 GeV (red) on the possible mass range of the lighter sbottom. As expected, this sensitivity degrades if the experimental central value for M_W goes down by 10 MeV (yellow points), which would bring it closer to the SM value given in Eq. (19). The right plot shows the results in the $m_{\tilde{b}_1}$–$m_{\tilde{t}_2}$ plane. It can be observed that sensitive upper bounds on those unknown particle masses could be set[9] based on an experimental value of M_W of 80.385 ± 0.005 GeV or 80.395 ± 0.005 GeV (i.e. for central values sufficiently different from the SM prediction). In this situation the precise M_W measurement could give interesting indications regarding the search for the heavy stop and the light sbottom (or put the interpretation within the MSSM under tension).

[9]See also Ref. [120] for a recent analysis investigating constraints on the scalar top sector.

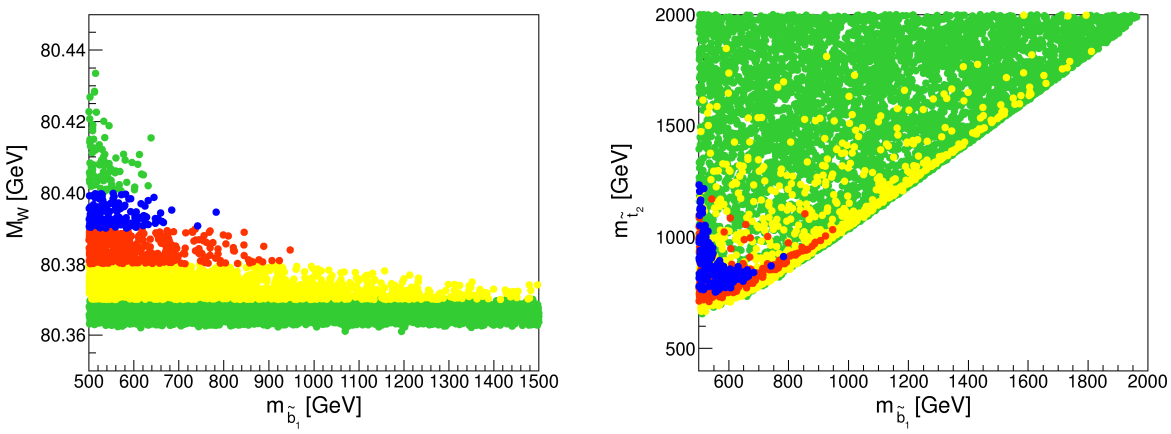


Figure 8: Results of an MSSM parameter scan illustrating the prediction for M_W in a hypothetical future scenario assuming a measurement of $m_{\tilde{t}_1} = 400 \pm 40$ GeV at the LHC as well as lower limits on all other SUSY particles: the assumed lower limits are 500 GeV for the other third generation squarks, 1200 GeV for all other colored particles, and 300 GeV for sleptons and charginos. All displayed points fulfill $M_h = 125.6 \pm 3.1$ GeV. The yellow, red and blue points correspond to $M_W = 80.375 \pm 0.005$ GeV (yellow), $M_W = 80.385 \pm 0.005$ GeV (red), and $M_W = 80.395 \pm 0.005$ GeV (blue). The left plot shows the prediction for M_W as a function of the lighter sbottom mass, $m_{\tilde{b}_1}$, while the right plot shows the M_W prediction in the $m_{\tilde{b}_1}$–$m_{\tilde{t}_2}$ plane.

6 Conclusions

We have presented the currently most precise prediction for the W boson mass in the MSSM and compared it with the state–of–the–art prediction in the SM. The evaluation in the MSSM includes the full one-loop result (for the general case of complex parameters) and all known higher-order corrections of SM and SUSY type. Within the SM, interpreting the signal discovered at the LHC as the SM Higgs boson with $M_H^{\rm SM} = 125.6$ GeV, there is no unknown parameter in the M_W prediction anymore. This yields $M_W^{\rm SM} = 80.361$ GeV, which is somewhat below (but compatible at the level of about $1.5\,\sigma$) with the current experimental value of $M_W^{\rm exp} = 80.385 \pm 0.015$ GeV. The loop contributions from supersymmetric particles in general give rise to an upward shift in the prediction for M_W as compared to the SM case, which tend to bring the prediction into better agreement with the experimental result. For very light superpartners of the top and bottom quarks and large mass splittings in this sector even much larger (and thus experimentally disfavored) values of M_W are possible.

We have investigated the MSSM and SM predictions in the M_W–m_t plane, updating earlier results in Ref. [17] while taking into account the existing constraints from Higgs and SUSY searches. We have analyzed in this context the implications of the results of present and possible future searches for supersymmetric particles at the LHC. While the existing bounds on the gluino and the squarks of the first two generations have only a minor effect, more stringent bounds on the third generation squarks would have a drastic

effect on the possible range of M_W values in the MSSM. In particular, assuming a lower bound of 500 GeV on the masses of the stops and sbottoms, the resulting range of predicted M_W values in the MSSM essentially reduces to the region that is best compatible with the experimental result (corresponding to the 68% C.L. region). We have shown that MSSM predictions in exact agreement with the current experimental central value of M_W can be reached for stop mass values as large as $m_{\tilde{t}_1} \sim 1.5$ TeV, even if all other SUSY particles are heavy. We have furthermore pointed out that even if the squarks are so heavy that their contribution to M_W becomes negligible, sizable SUSY contributions to M_W are nevertheless possible if either charginos, neutralinos or sleptons are light. Analyzing the impact of light SUSY particles that are still allowed by LHC searches we have found that scalar leptons can give a contribution larger than 60 MeV, while light charginos can give corrections of up to ~ 20 MeV.

Besides the impact of limits from searches for supersymmetric particles, we have analyzed the constraints arising from the Higgs signal at about 125.6 GeV. Within the MSSM this signal can be interpreted, at least in principle, either as the light or the heavy $\mathcal{CP}$-even Higgs boson (we have not addressed here the possibility of a state consisting of an admixture of $\mathcal{CP}$-even and $\mathcal{CP}$-odd components). Concerning the interpretation in terms of the light $\mathcal{CP}$-even Higgs boson, the result for M_W turns out to be well compatible with the additional constraint that M_h should be in the mass range compatible with the signal. The main effect of this constraint is that it somewhat reduces the allowed range of predicted M_W values in the MSSM, improving in this way the overall compatibility with the experimental result for M_W. It is remarkable that also the rather exotic scenario where the mass of the heavy $\mathcal{CP}$-even Higgs boson is required to be in the range compatible with the observed signal (which is under pressure in particular from the recent ATLAS bound on light charged Higgs bosons) leads to predicted values for M_W that tend to be in better agreement with the experimental result than for the SM case. It is interesting to note that in this case, which corresponds to an MSSM scenario outside of the decoupling region, there is no overlap between the SM prediction and the range of MSSM predictions for M_W. A high-precision measurement of M_W could thus yield a clear distinction between the two models in such a scenario.

As another interesting feature in the context of Higgs phenomenology, we have studied the correlation between M_W and $\Gamma(h \to \gamma\gamma)$ via light scalar taus. Light staus contribute to the loop-induced process $h \to \gamma\gamma$, leading to an enhancement of the $\gamma\gamma$ width over the SM prediction. At the same time staus appear in the MSSM loop corrections to the muon decay, and thus light staus can also yield a sizable contribution to the prediction for M_W. We have demonstrated that light staus can have the simultaneous effect of enhancing $\Gamma(h \to \gamma\gamma)$ while bringing the M_W prediction in perfect agreement with the current experimental central value of M_W.

As a final step we have discussed the impact of the precision observable M_W in the context of possible future scenarios. The improved precision on M_W and m_t from future measurements at the LHC and in particular at a prospective Linear Collider (ILC) would significantly enhance the sensitivity to discriminate between the SM and the MSSM (as well as other BSM scenarios). Analyzing in this context the impact of possible future LHC results in the stop sector on the M_W prediction, we have discussed a hypothetical scenario where a light stop has been detected at the LHC, while lower limits have been imposed on all other SUSY particles. We have demonstrated that, depending on the future central experimental

value, a high-precision measurement of M_W could yield quite stringent *upper* bounds on the mass of the heavier stop and the lighter sbottom, which could be of great interest regarding the direct searches for those particles. In case other SUSY particles were detected, this would further sharpen the sensitivity for determining unknown mass scales of the model.

Acknowledgements

We are grateful to A. Freitas, T. Hahn, A. Kotwal, O. Stål, T. Stefaniak and D. Wackeroth for helpful discussions. This work has been supported by the Collaborative Research Center SFB676 of the DFG, "Particles, Strings and the early Universe". The work of S.H. was supported in part by CICYT (grant FPA 2010–22163-C02-01) and by the Spanish MICINN's Consolider-Ingenio 2010 Program under grant MultiDark CSD2009-00064.

References

[1] ATLAS Collaboration, G. Aad *et. al. Phys.Lett.* **B716** (2012) 1–29, [arXiv:1207.7214].

[2] CMS Collaboration, S. Chatrchyan *et. al. Phys.Lett.* **B716** (2012) 30–61, [arXiv:1207.7235].

[3] CDF Collaboration, T. Aaltonen *et. al.* [arXiv:1203.0275].

[4] DØ Collaboration, V. M. Abazov *et. al.* [arXiv:1203.0293].

[5] ALEPH Collaboration, DELPHI Collaboration, L3 Collaboration, OPAL Collaboration, LEP Electroweak Working Group, J. Alcaraz *et. al.* [hep-ex/0612034].

[6] Tevatron Electroweak Working Group [arXiv:1204.0042].

[7] ALEPH Collaboration, DELPHI Collaboration, L3 Collaboration, OPAL Collaboration, SLD Collaboration, LEP Electroweak Working Group, SLD Electroweak Group, SLD Heavy Flavour Group, S. Schael *et. al. Phys.Rept.* **427** (2006) 257–454, [hep-ex/0509008], see: http://lepewwg.web.cern.ch/LEPEWWG/.

[8] S. Heinemeyer, S. Kraml, W. Porod, and G. Weiglein *JHEP* **0309** (2003) 075, [hep-ph/0306181].

[9] S. Heinemeyer and G. Weiglein [arXiv:1007.5232].

[10] D. Stöckinger *J.Phys.* **G34** (2007) R45–R92, [hep-ph/0609168].

[11] J. P. Miller, E. d. Rafael, B. L. Roberts, and D. Stöckinger *Ann.Rev.Nucl.Part.Sci.* **62** (2012) 237–264.

[12] F. Jegerlehner and A. Nyffeler *Phys.Rept.* **477** (2009) 1–110, [arXiv:0902.3360].

[13] Heavy Flavor Averaging Group, Y. Amhis *et. al.* [arXiv:1207.1158], see: http://www.slac.stanford.edu/xorg/hfag.

[14] H. P. Nilles *Phys.Rept.* **110** (1984) 1–162.

[15] H. E. Haber and G. L. Kane *Phys.Rept.* **117** (1985) 75–263.

[16] R. Barbieri *Riv.Nuovo Cim.* **11N4** (1988) 1–45.

[17] S. Heinemeyer, W. Hollik, D. Stöckinger, A. M. Weber, and G. Weiglein *JHEP* **08** (2006) 052, [hep-ph/0604147].

[18] S. Heinemeyer, W. Hollik, and G. Weiglein *Phys.Rept.* **425** (2006) 265–368, [hep-ph/0412214].

[19] S. Heinemeyer, W. Hollik, F. Merz, and S. Penaranda *Eur.Phys.J.* **C37** (2004) 481–493, [hep-ph/0403228].

[20] O. Stål, G. Weiglein, and L. Zeune, in preparation.

[21] F. Domingo and T. Lenz *JHEP* **1107** (2011) 101, [arXiv:1101.4758].

[22] M. Awramik, M. Czakon, and A. Freitas *JHEP* **11** (2006) 048, [hep-ph/0608099].

[23] P. Z. Skands and D. Wicke *Eur.Phys.J.* **C52** (2007) 133–140, [hep-ph/0703081].

[24] A. H. Hoang and I. W. Stewart *Nucl.Phys.Proc.Suppl.* **185** (2008) 220–226, [arXiv:0808.0222].

[25] J. Boyd, talk given at SUSY2013, see: http://susy2013.ictp.it/lecturenotes/03_Wednesday/Boyd.pdf.

[26] J. Richman, talk given at SUSY2013, see: http://susy2013.ictp.it/lecturenotes/03_Wednesday/Richman.pdf.

[27] ATLAS Collaboration, see: https://twiki.cern.ch/twiki/bin/view/AtlasPublic/SupersymmetryPublicResults.

[28] CMS Collaboration, see: https://twiki.cern.ch/twiki/bin/view/CMSPublic/PhysicsResultsSUS.

[29] T. J. LeCompte and S. P. Martin *Phys.Rev.* **D84** (2011) 015004, [arXiv:1105.4304].

[30] R. Mahbubani, M. Papucci, G. Perez, J. T. Ruderman, and A. Weiler [arXiv:1212.3328].

[31] Particle Data Group, J. Beringer *et. al. Phys.Rev.* **D86** (2012) 010001, and 2013 partial update for the 2014 edition.

[32] S. Heinemeyer, O. Stål, and G. Weiglein *Phys.Lett.* **B710** (2012) 201–206, [arXiv:1112.3026].

[33] M. Carena, S. Heinemeyer, O. Stl, C. Wagner, and G. Weiglein *Eur. Phys. J.* **C73** (2013) 2552, [arXiv:1302.7033].

[34] P. Bechtle, S. Heinemeyer, O. Stal, T. Stefaniak, G. Weiglein, *et. al. Eur.Phys.J.* **C73** (2013) 2354, [arXiv:1211.1955].

[35] A. Bottino, N. Fornengo, and S. Scopel *Phys.Rev.* **D85** (2012) 095013, [arXiv:1112.5666].

[36] M. Drees *Phys.Rev.* **D86** (2012) 115018, [arXiv:1210.6507].

[37] K. Hagiwara, J. S. Lee, and J. Nakamura *JHEP* **1210** (2012) 002, [arXiv:1207.0802].

[38] A. Arbey, M. Battaglia, A. Djouadi, and F. Mahmoudi *JHEP* **1209** (2012) 107, [arXiv:1207.1348].

[39] ATLAS Collaboration, ATLAS-CONF-2013-090.

[40] P. Bechtle, O. Brein, S. Heinemeyer, O. Stål, T. Stefaniak, *et. al.* [arXiv:1301.2345].

[41] P. Bechtle, O. Brein, S. Heinemeyer, G. Weiglein, and K. E. Williams *Comput.Phys.Commun.* **182** (2011) 2605–2631, [arXiv:1102.1898].

[42] P. Bechtle, O. Brein, S. Heinemeyer, G. Weiglein, and K. E. Williams *Comput.Phys.Commun.* **181** (2010) 138–167, [arXiv:0811.4169].

[43] P. Bechtle, O. Brein, S. Heinemeyer, O. Stål, T. Stefaniak, *et. al.* [arXiv:1311.0055].

[44] M. Arana-Catania, S. Heinemeyer, M. Herrero, and S. Penaranda *JHEP* **1205** (2012) 015, [arXiv:1109.6232].

[45] MuLan Collaboration, D. Webber *et. al. Phys.Rev.Lett.* **106** (2011) 041803, [arXiv:1010.0991].

[46] R. Behrends, R. Finkelstein, and A. Sirlin *Phys.Rev.* **101** (1956) 866–873.

[47] T. Kinoshita and A. Sirlin *Phys.Rev.* **113** (1959) 1652–1660.

[48] T. van Ritbergen and R. G. Stuart *Nucl.Phys.* **B564** (2000) 343–390, [hep-ph/9904240].

[49] M. Steinhauser and T. Seidensticker *Phys.Lett.* **B467** (1999) 271–278, [hep-ph/9909436].

[50] A. Pak and A. Czarnecki *Phys.Rev.Lett.* **100** (2008) 241807, [arXiv:0803.0960].

[51] A. Sirlin *Phys.Rev.* **D22** (1980) 971–981.

[52] A. Freitas, W. Hollik, W. Walter, and G. Weiglein *Nucl.Phys.* **B632** (2002) 189–218, [hep-ph/0202131], [Erratum-ibid. **B666** (2003) 305-307].

[53] W. Marciano and A. Sirlin *Phys.Rev.* **D22** (1980) 2695.

[54] A. Djouadi and C. Verzegnassi *Phys. Lett.* **B195** (1987) 265.

[55] A. Djouadi *Nuovo Cim.* **A100** (1988) 357.

[56] B. Kniehl *Nucl. Phys.* **B347** (1990) 86.

[57] F. Halzen and B. Kniehl *Nucl. Phys.* **B353** (1991) 567.

[58] B. Kniehl and A. Sirlin *Nucl. Phys.* **B371** (1992) 141.

[59] B. Kniehl and A. Sirlin *Phys. Rev.* **D47** (1993) 883.

[60] A. Freitas, W. Hollik, W. Walter, and G. Weiglein *Phys.Lett.* **B495** (2000) 338–346, [hep-ph/0007091], [Erratum-ibid. **B570** (2003) 260-264].

[61] M. Awramik and M. Czakon *Phys. Lett.* **B568** (2003) 48, [hep-ph/0305248].

[62] M. Awramik and M. Czakon *Phys. Rev. Lett.* **89** (2002) 241801, [hep-ph/0208113].

[63] A. Onishchenko and O. Veretin *Phys. Lett.* **B551** (2003) 111, [hep-ph/0209010].

[64] M. Awramik, M. Czakon, A. Onishchenko, and O. Veretin *Phys. Rev.* **D68** (2003) 053004, [hep-ph/0209084].

[65] L. Avdeev, J. Fleischer, S. Mikhailov, and O. Tarasov *Phys.Lett.* **B336** (1994) 560, [hep-ph/9406363].

[66] K. G. Chetyrkin, J. H. Kühn, and M. Steinhauser *Phys. Lett.* **B351** (1995) 331, [hep-ph/9502291].

[67] K. G. Chetyrkin, J. Kühn, and M. Steinhauser *Phys. Rev. Lett.* **75** (1995) 3394, [hep-ph/9504413].

[68] K. Chetyrkin, J. Kühn, and M. Steinhauser *Nucl.Phys.* **B482** (1996) 213, [hep-ph/9606230].

[69] M. Faisst, J. H. Kühn, T. Seidensticker, and O. Veretin *Nucl. Phys.* **B665** (2003) 649, [hep-ph/0302275].

[70] K. Chetyrkin, M. Faisst, J. H. Kühn, P. Maierhofer, and C. Sturm *Phys.Rev.Lett.* **97** (2006) 102003, [hep-ph/0605201].

[71] R. Boughezal and M. Czakon *Nucl.Phys.* **B755** (2006) 221, [hep-ph/0606232].

[72] J. van der Bij, K. Chetyrkin, M. Faisst, G. Jikia, and T. Seidensticker *Phys.Lett.* **B498** (2001) 156–162, [hep-ph/0011373].

[73] R. Boughezal, J. Tausk, and J. van der Bij *Nucl.Phys.* **B713** (2005) 278–290, [hep-ph/0410216].

[74] M. Awramik, M. Czakon, A. Freitas, and G. Weiglein *Phys.Rev.* **D69** (2004) 053006, [hep-ph/0311148].

[75] R. Barbieri and L. Maiani *Nucl.Phys.* **B224** (1983) 32.

[76] C. Lim, T. Inami, and N. Sakai *Phys.Rev.* **D29** (1984) 1488.

[77] E. Eliasson *Phys.Lett.* **B147** (1984) 65.

[78] Z. Hioki *Prog.Theor.Phys.* **73** (1985) 1283.

[79] J. Grifols and J. Sola *Nucl.Phys.* **B253** (1985) 47.

[80] R. Barbieri, M. Frigeni, F. Giuliani, and H. Haber *Nucl.Phys.* **B341** (1990) 309–321.

[81] M. Drees and K. Hagiwara *Phys.Rev.* **D42** (1990) 1709–1725.

[82] M. Drees, K. Hagiwara, and A. Yamada *Phys.Rev.* **D45** (1992) 1725–1743.

[83] P. H. Chankowski, A. Dabelstein, W. Hollik, W. Mosle, S. Pokorski, and J. Rosiek *Nucl.Phys.* **B417** (1994) 101.

[84] D. Garcia and J. Sola *Mod.Phys.Lett.* **A9** (1994) 211–224.

[85] D. M. Pierce, J. A. Bagger, K. T. Matchev, and R.-j. Zhang *Nucl.Phys.* **B491** (1997) 3–67, [hep-ph/9606211].

[86] A. Djouadi, P. Gambino, S. Heinemeyer, W. Hollik, C. Junger, and G. Weiglein *Phys.Rev.Lett.* **78** (1997) 3626, [hep-ph/9612363].

[87] A. Djouadi, P. Gambino, S. Heinemeyer, W. Hollik, C. Junger, and G. Weiglein *Phys.Rev.* **D57** (1998) 4179, [hep-ph/9710438].

[88] S. Heinemeyer and G. Weiglein *JHEP* **0210** (2002) 072, [hep-ph/0209305].

[89] J. Haestier, S. Heinemeyer, D. Stöckinger, and G. Weiglein *JHEP* **0512** (2005) 027, [hep-ph/0508139].

[90] Wolfram Research, Inc., Mathematica, Version 8.0, Champaign, IL (2010).

[91] J. Küblbeck, M. Böhm, and A. Denner *Comput.Phys.Commun.* **60** (1990) 165–180.

[92] A. Denner, H. Eck, O. Hahn, and J. Küblbeck *Phys.Lett.* **B291** (1992) 278–280.

[93] A. Denner, H. Eck, O. Hahn, and J. Küblbeck *Nucl.Phys.* **B387** (1992) 467–484.

[94] J. Küblbeck, H. Eck, and R. Mertig *Nucl.Phys.Proc.Suppl.* **29A** (1992) 204–208.

[95] T. Hahn *Comput.Phys.Commun.* **140** (2001) 418, [hep-ph/0012260].

[96] T. Hahn and C. Schappacher *Comput.Phys.Commun.* **143** (2002) 54–68, [hep-ph/0105349].

[97] T. Hahn and M. Perez-Victoria *Comput.Phys.Commun.* **118** (1999) 153, [hep-ph/9807565].

[98] M. Veltman *Nucl.Phys.* **B123** (1977) 89.

[99] M. Consoli, W. Hollik, and F. Jegerlehner *Phys.Lett.* **B227** (1989) 167.

[100] R. Barbieri, M. Beccaria, P. Ciafaloni, G. Curci, and A. Vicere *Nucl.Phys.* **B409** (1993) 105–127.

[101] J. Fleischer, O. Tarasov, and F. Jegerlehner *Phys.Lett.* **B319** (1993) 249–256.

[102] T. Hahn, S. Heinemeyer, W. Hollik, H. Rzehak, and G. Weiglein *Comput.Phys.Commun.* **180** (2009) 1426–1427.

[103] M. Frank, T. Hahn, S. Heinemeyer, W. Hollik, H. Rzehak, *et. al. JHEP* **0702** (2007) 047, [hep-ph/0611326].

[104] G. Degrassi, S. Heinemeyer, W. Hollik, P. Slavich, and G. Weiglein *Eur.Phys.J.* **C28** (2003) 133–143, [hep-ph/0212020].

[105] S. Heinemeyer, W. Hollik, and G. Weiglein *Eur.Phys.J.* **C9** (1999) 343–366, [hep-ph/9812472].

[106] S. Heinemeyer, W. Hollik, and G. Weiglein *Comput.Phys.Commun.* **124** (2000) 76–89, [hep-ph/9812320].

[107] ATLAS Collaboration ATLAS-CONF-2013-014, ATLAS-COM-CONF-2013-025.

[108] CMS Collaboration CMS-PAS-HIG-13-005.

[109] R. Hempfling *Phys.Rev.* **D49** (1994) 6168–6172.

[110] L. J. Hall, R. Rattazzi, and U. Sarid *Phys.Rev.* **D50** (1994) 7048–7065, [hep-ph/9306309].

[111] M. S. Carena, M. Olechowski, S. Pokorski, and C. Wagner *Nucl.Phys.* **B426** (1994) 269–300, [hep-ph/9402253].

[112] M. S. Carena, D. Garcia, U. Nierste, and C. E. Wagner *Nucl.Phys.* **B577** (2000) 88–120, [hep-ph/9912516].

[113] O. Stål and G. Weiglein *JHEP* **1201** (2012) 071, [arXiv:1108.0595].

[114] M. Carena, S. Gori, N. R. Shah, C. E. Wagner, and L.-T. Wang *JHEP* **1207** (2012) 175, [arXiv:1205.5842].

[115] M. Carena, S. Gori, N. R. Shah, and C. E. Wagner *JHEP* **1203** (2012) 014, [arXiv:1112.3336].

[116] ATLAS Collaboration ATLAS-CONF-2013-012.

[117] CMS Collaboration CMS-PAS-HIG-13-001.

[118] M. Baak, A. Blondel, A. Bodek, R. Caputo, T. Corbett, *et. al.* [arXiv:1310.6708].

[119] H. Baer, T. Barklow, K. Fujii, Y. Gao, A. Hoang, *et. al.* [arXiv:1306.6352].

[120] V. Barger, P. Huang, M. Ishida, and W.-Y. Keung *Phys.Lett.* **B718** (2013) 1024–1030, [arXiv:1206.1777].